NASA Technical Memorandum 87298
AIAA–86–1627

A Numerical Analysis Applied to High Angle of Attack Three-Dimensional Inlets

Danny P. Hwang
Lewis Research Center
Cleveland, Ohio

Prepared for the
22nd Joint Propulsion Conference
cosponsored by the AIAA, ASME, SAE, and ASEE
Huntsville, Alabama, June 16–18, 1986

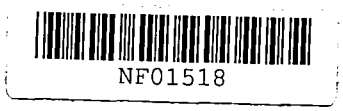

A NUMERICAL ANALYSIS APPLIED TO HIGH ANGLE OF ATTACK THREE-DIMENSIONAL INLETS

Danny P. Hwang
National Aeronautics and Space Administration
Lewis Research Center
Cleveland, Ohio 44135

Abstract

The three-dimensional analytical methods used to analyze subsonic high angle of attack inlets at the NASA Lewis Research Center are briefly described. The methods are then shown to give good agreement with experimental results for various three-dimensional high angle of attack inlets. Finally, because of this good agreement, the methods have been used to predict aerodynamic characteristics of scarf and slotted-lip inlets. Results of this analytical study are presented.

Nomenclature

L	inlet length
M_0	free stream Mach number
M_T	throat Mach number
ΔM	the difference of maximum Mach number between slat and cowl
$\dot{m}$	mass flow rate
p_s	static pressure
P_t	free stream total pressure
R_2	Internal cowl radius at fan face = 0.254 m
S	surface distance from highlight
V_t	throat velocity
X	axial distance
α	angle of attack
β	angle of yaw

Introduction

In recent years, there has been an increasing interest in the development of a high performance propulsion system for V/STOL and highly maneuverable aircraft. Some of the proposed concepts are non-axisymmetric, as shown in Fig. 1, and impose very high angle of attack requirements on the propulsion system's inlet. Separation-free flow at these severe operating conditions is a major concern for the designer in achieving a high performance system.

There are many ideas proposed for the design of a high angle-of-attack inlet. One example is a thick lip axisymmetric inlet that has a contraction ratio of 1.46.[1] Another example is an asymmetric inlet that has an overall contraction ratio of 1.5, whereas the local contraction ratio of the leeward cowl is 1.3 and that of the windward cowl is 1.76.[2] Another concept is a scarf inlet[3] that is characterized by having a longer lower lip than an upper lip. A slotted-lip inlet that has either a single slat or double slats in front of the inlet[4] has also been suggested. This paper only covers the four concepts mentioned above. Other ideas, such as blowing and suction boundary layer controls used to prevent separation[5-8] are not included in this study.

Basic Method of Analysis

The series of three-dimensional panel method and two-dimensional boundary layer programs used at NASA Lewis for subsonic inlet analysis are depicted in Fig. 2. A geometry program creates the discrete three-dimensional control points for each geometric configuration. Then, a three-dimensional imcompressible potential flow program[9-11] is used to calculate the basic solutions to the problem. The basic solutions consist of a static solution (i.e., $V_0 = 0$), and the solutions which determine the flow about the inlet due to a unit free stream velocity at prescribed angle of attack and yaw with no effort to control mass flow through the inlet.[11] These basic solutions are combined into one that satisfies velocity, angle of attack, and inlet mass flow. Next, the resulting incompressible flow solution is corrected for compressibility effects by the method of Lieblien and Stockman.[12] The compressible potential flow solution is then used as an input to the Herring's boundary-layer program[13] to calculate the skin friction coefficient which in turn is used as an indicator of flow separation when the coefficient reaches zero.

For the present study, no attempt has been made to correct the displacement thickness on the input geometry surface. As shown in Fig. 2, there is an iteration loop to find the separation angle of attack of an inlet at any given value of free stream velocity and inlet mass flow in one uninterrupted computer run.

Comparison of Analytical and Experimental Results

The result of the three-dimensional potential flow calculation with compressibility correction along with experimental results for an axisymmetric thick-lip inlet are shown in Fig. 3. Figure 4 shows the internal static pressure distribution on the inlet windward surface at various mass flow rates for an asymmetric inlet. Axial distribution of surface static pressure on inlet leeward side for a scarf inlet is given in Fig. 5. The agreement with experiment for all above inlets are excellent.

Figure 6(a) shows comparison of the analytical predictions and the experimental results in terms of the surface Mach number for a slotted-lip inlet. The difference between analysis and experiment at point A in the figure will be discussed later. The similar trend is shown for $\alpha = 40°$ as given in Fig. 6(b).

The separation angle of attack of the inlet is defined as the highest angle of attack at which the flow at the fan face remains attached. The separation angle of attack is predicted when the skin friction coefficient along the most adverse streamtube calculated by the boundary layer program becomes zero. The separation bounds of a scarf inlet and an asymmetric inlet are shown in Fig. 7 and 8. The agreement between analysis and experiment for both inlets are quite good. Figure 9 is another illustration of good agreement between analysis and experiment in terms of ΔM, the difference of the maximum Mach number between slat and cowl.

Application of Analytical Method

The present analytical method was first applied to a scarf inlet in order to study the effect of inlet rotation on the separation bound. Three positions were considered, i.e., the normal position having the longer lip at the windward plane, the upside-down position having the shorter lip at the windward plane and the sideway position having the inlet rotated 90° from normal position. As shown in Fig. 10, the normal position had a higher separation bound than the other two positions by a large margin. The reason why it performed so well in the normal position was explained in a report[3] presenting experimental results. For sideway position, the stream line was traced at 135° from windward plane, because the diffusion ratio is the highest at that circumferential position and flow separation is most likely to occur there, as indicated in Fig. 11. A dashed line in Fig. 11 indicates a constant Mach number line of 1.5. If the local Mach number is beyond 1.5, the flow most likely separates due to shock and boundary layer interaction. The current method can not predict this type of separation.

The method was then applied to a slotted-lip inlet. Figure 12 shows the effect of free stream Mach number on the surface Mach number of the inlet. As indicated in the figure, the increase in free stream Mach number will increase Mach number at point B (leading edge of the slat). Due to abrupt diffusion at point B, flow most likely separates there. This type of separation is not considered in the current calculation. This error of not accommodating the separated region in the calculation could have been responsible for the difference shown in Fig. 6, especially at point A.

In the same figure, it can be noticed that while the stagnation point, point D, on the cowl moves forward when the free stream Mach number is increased, the flow around point C remains practically unchanged. This is because point C is close to the fan face, therefore the flow around point C is dominated by the fan face flow rate. The Mach number on the slat is very sensitive to the change in free stream Mach number. As indicated in Fig. 12, free stream Mach number was increased from 0.065 to 0.13, which is equivalent to the change of 0.0088 in static to total pressure ratio. This small change is almost within the range of the error which could be introduced during the measurement. The difference shown at point A in Fig. 6 could be the disagreement between analysis and experiment in free stream Mach number value. Also notice that when free stream Mach number is increased, the loading at point A is reduced while the loading at point B is increased.

The effect of gap size on surface Mach number is illustrated in Fig. 13. The loading is decreased on the slat and increased on the cowl when gap size is increased. In other words, the Mach number at point A decreases while the Mach numbers at point C increases when gap size is increased. As mentioned previously, the leading edge of the slat, point B, is so sharp that the flow could separate there. Once the flow separates at the leading edge of the slat, the effective gap size and the slat thickness are changed drastically due to the boundary layer built-up on the surface. The difference of maximum Mach number at point A in Fig. 6 could be partially due to the difference in the "effective" gap size of the experiment and the input gap size of the analysis.

As expected, the effect of angle of attack on the surface Mach number at the windward plane is the increase in Mach number on both slat and cowl as indicated in Fig. 14.

An attempt has been made to optimize gap size of a slotted-lip inlet. The design point of Refs. 4 and 7, i.e., $V_0 = 27.7$ m/sec, $V_t = 35.5$ m/sec and $\alpha = 70°$, was used for optimization. The design point is the most severe flow condition under the V/STOL flight envelope. If the flow does not separate here, it will remain attached everywhere during the flight. The optimized gap size is reached when the maximum Mach numbers on the slat and the cowl are equal, i.e., $\Delta M = 0$, so that both have the same diffusion. ΔM is plotted against gap size in Fig. 15, and the optimized gap size is found to be 1.65 cm for this particular slat.

The separation bounds of axisymmetric inlet, asymmetric inlet, scarf inlet and slotted-lip inlet are summarized in Fig. 16. The slotted-lip inlet has the highest separation bound. Analytical calculation of separation bound for this inlet is very difficult because angle of attack is larger than 80° and it is hard to determine whether separation occurs on the slat first or on the cowl first. However, separation bound found by experiment was shown in Fig. 16 for comparison. An asymmetric inlet is slightly better than a scarf inlet and both perform much better than an axisymmetric thick lip inlet.

Concluding Remarks

Three-dimensional analytical investigations based on three-dimensional panel methods and two-dimensional boundary layer programs were conducted to evaluate the accuracy of the method. The results of the investigation can be summarized as follows:

1. The three-dimensional analytical methods used to study three-dimensional inlets at NASA Lewis agree well with experimental results for an axisymmetric inlet, an asymmetric inlet and a scarf inlet.

2. A slight difference between analysis and experiment in surface Mach number of the slat could be the combined effect of many factors:

a) Neglect the possible flow separation at the leading edge of the slat in analysis study.

b) The surface Mach number is very sensitive to the free stream Mach number. A small error in the measurement of free stream Mach number could contribute to the difference between analysis and experiment.

c) The flow separation at the slat leading edge could change the effective gap size between slat and cowl. The gap size used in analysis could be somewhat different from the effective gap size of the experiment.

d) The difference could be partially due to the accuracy of the analysis method.

3. Three different positions of a scarf inlet were investigated, and the separation bound was the best for the position having the longer lip at windward plane.

4. The aerodynamic analysis was conducted for a slotted-lip inlet, and the optimum gap size was found to be 1.64 cm for the particular slat under study.

5. Among the presented concepts, the separation bound is the highest for an slotted-lip inlet, and the lowest for an axisymmetric inlet. The separation bound of an asymmetric inlet is slightly higher than that of a scarf inlet for higher V_T/V_0 values.

Reference

1. Miller, B.A., Dastoli, B.J., and Wesoky, H.L., "Effect of Entry-Lip Design on Aerodynamics and Acoustics of High-Throat Mach Number Inlets for the Quiet, Clean, Short-Haul Experimental Engine," NASA TM-X-3222, 1975.

2. Koncsek, J.L., and Shaw, R.J., "Operating Characteristics of an Inlet Model Tested with a 0.5 m Powered Fan at High Angles of Attack," NASA CR-135270, 1977.

3. Abbott, J.M., "Aerodynamic Performance of Scarf Inlets," AIAA Paper 79-0380, Jan. 1979.

4. Woollett, R.R., Beck, W.E., Jr. and Glasgow, E.R., "Wind Tunnel Tests of a Zero-Length, Slotted-Lip Engine Air Inlet for a Fixed Nacelle V/STOL Aircraft," NASA TM-82939, 1980.

5. Hwang, D.P., and Abbott, J.M., "A Summary of V/STOL Inlet Analysis Methods," ICAS Proceedings 1982, Vol. I, AIAA, New York, 1982, pp. 402-409.

6. Burley, R.R, and Hwang, D.P., "Investigation of Tangential Blowing Applied to a Subsonic V/STOL Inlet," Journal of Aircraft, Vol. 20, No. 11, Nov. 1983, pp. 926-934.

7. Hwang, D.P., "Analytical Study of Blowing Boundary Layer Control for Subsonic V/STOL Inlets," Computations of Internal Flows: Methods and Applications, ASME FED-14, ASME, New York, 1983, pp. 151-157.

8. Boles, M.A., Ramesh, K., and Hwang, D.P., "Analytical Study of Suction Boundary Layer Control for Subsonic V/STOL Inlets," AIAA Paper 84-1399, June 1984.

9. Hess, J.L., Mack, D.P., and Stockman, N.O., "An Efficient User-Oriented Method for Calculating Compressible Flow In and About Three-Dimensional Inlets," Douglas Aircraft Co., Long Beach, CA, MDC-J7733, Apr. 1979. (NASA CR-159578).

10. Hess, J.L., and Friedman, D.M., "Calculation of Compressible Flow In and About Three-Dimensional Inlets With and Without Auxiliary Inlets by a Higher-Order Panel Method," Douglas Aircraft Co., Long Beach, CA, MDC-J2548, Oct. 1982 (NASA CR-168009).

11. Hess, J.L., and Friedman, D.M., and Clark, R.W., "Calculation of Compressible Flow About Three-Dimensional Inlets with Auxiliary Inlets, Slats and Vanes by Means of a Panel Method," Douglas Aircraft Co., Long Beach, CA, MDC-J3789, June, 1985. (NASA CR-174975).

12. Lieblien, S., and Stockman, N.O., "Compressibility Correction for Internal Flow Solutions," Journal of Aircraft, Vol. 9, No. 4, Apr. 1972, pp. 312-313.

13. Herring, H.J., "PL2 - A Calculation Method for Two-Dimensional Boundary Layers with Crossflow and Heat Transfer," Dynalysis of Princeton, Princeton, NJ, Report No. 65, July 1980.

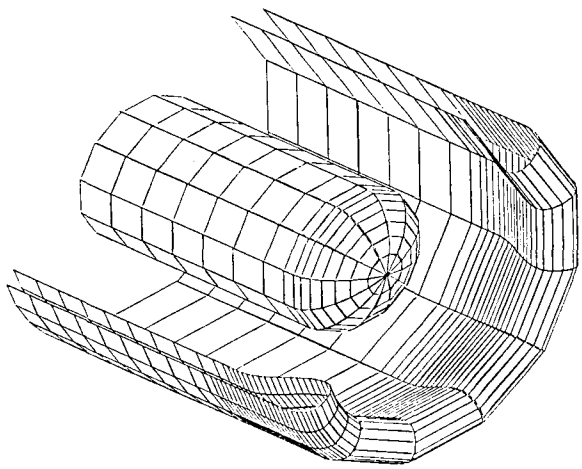

AXISYMMETRIC THICK LIP INLET

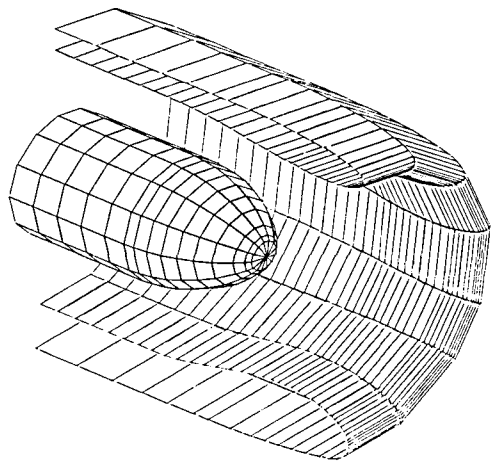

ASYMMETRIC INLET

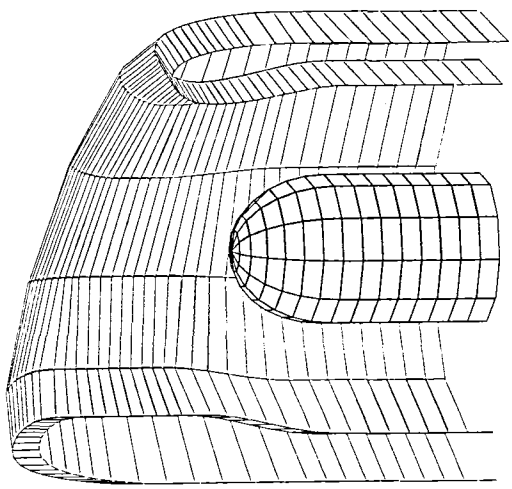

SCARF INLET

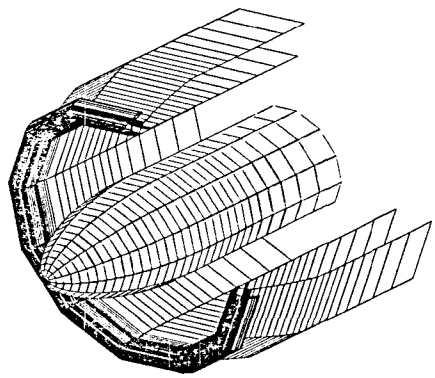

INLET WITH SINGLE SLAT

Figure 1. - Geometries of high angle of attack inlets.

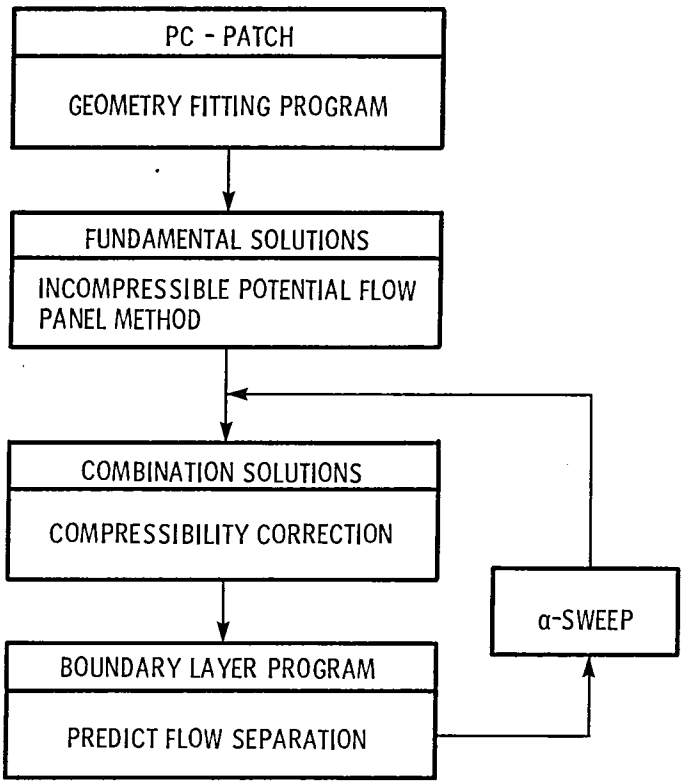

Figure 2. - 3-D inviscid - viscous analysis method.

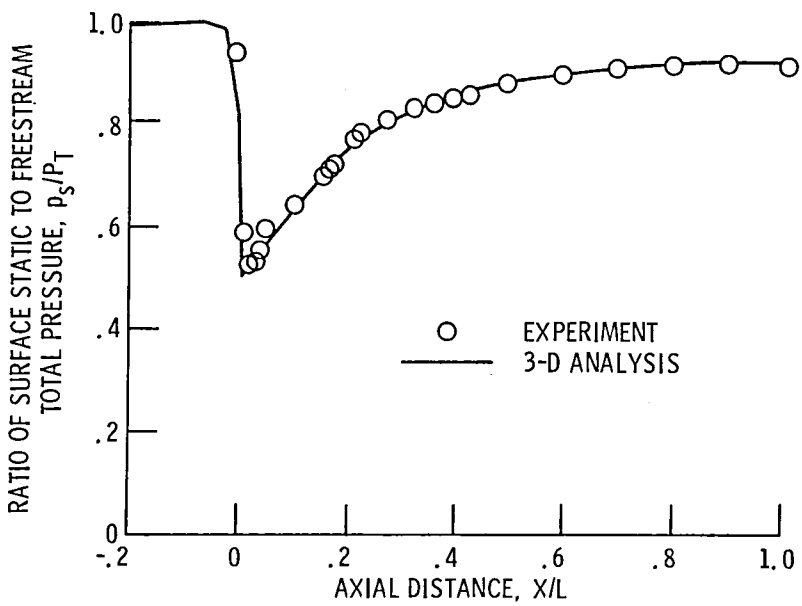

Figure 3. - Comparison of 3-D analysis and experiment, axisymmetric thick lip inlet. ($\alpha = 39.66^0$; $M_0 = 0.182$; $M_T = 0.47$.)

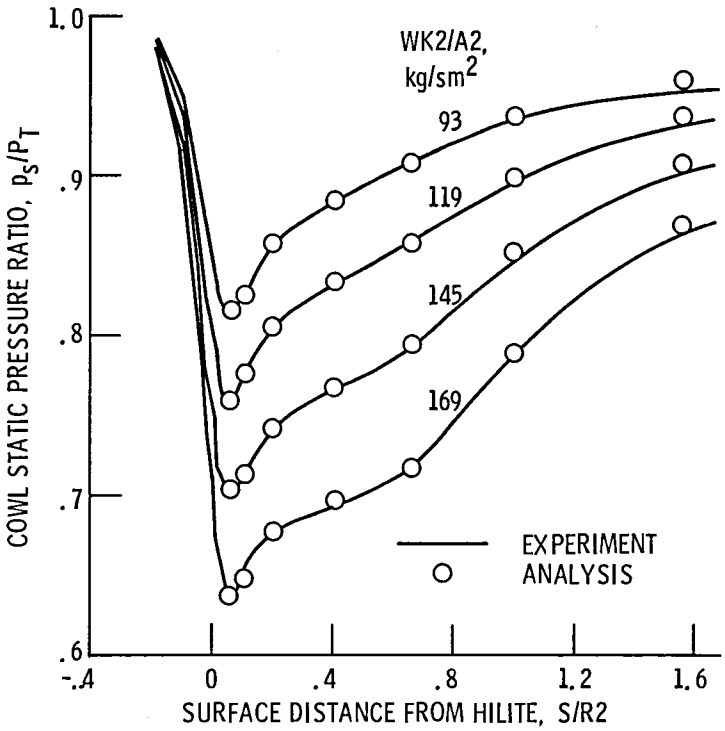

Figure 4. - Comparison of 3-D analysis and experiment, asymmetric inlet. ($\alpha = 60^0$; $M_0 = 0.12$.)

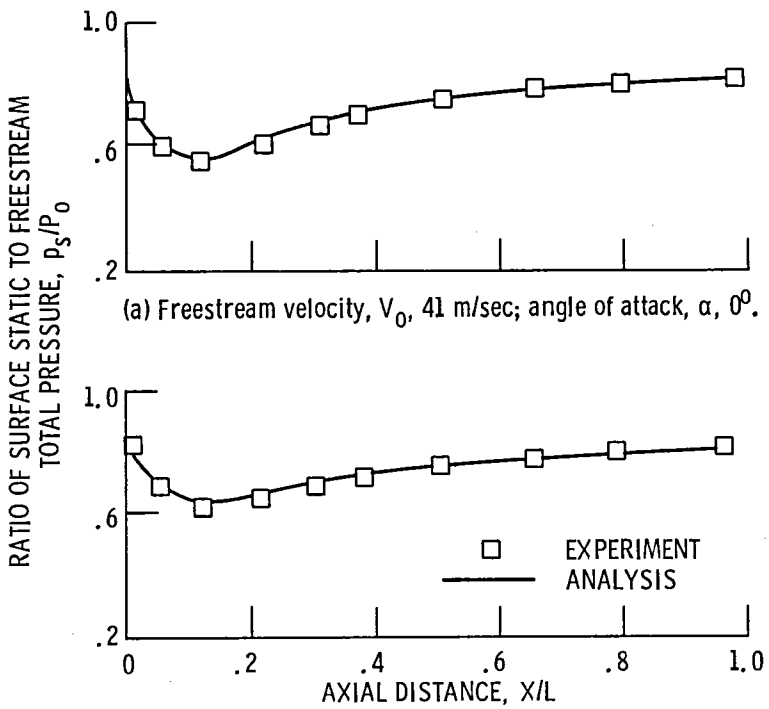

(a) Freestream velocity, V_0, 41 m/sec; angle of attack, α, 0^0.

(b) Freestream velocity, V_0, 41 m/sec; angle of attack, α, 50^0.

Figure 5. - Axial distribution of surface static pressure on inlet leeward side. ($M_T = 0.54$.)

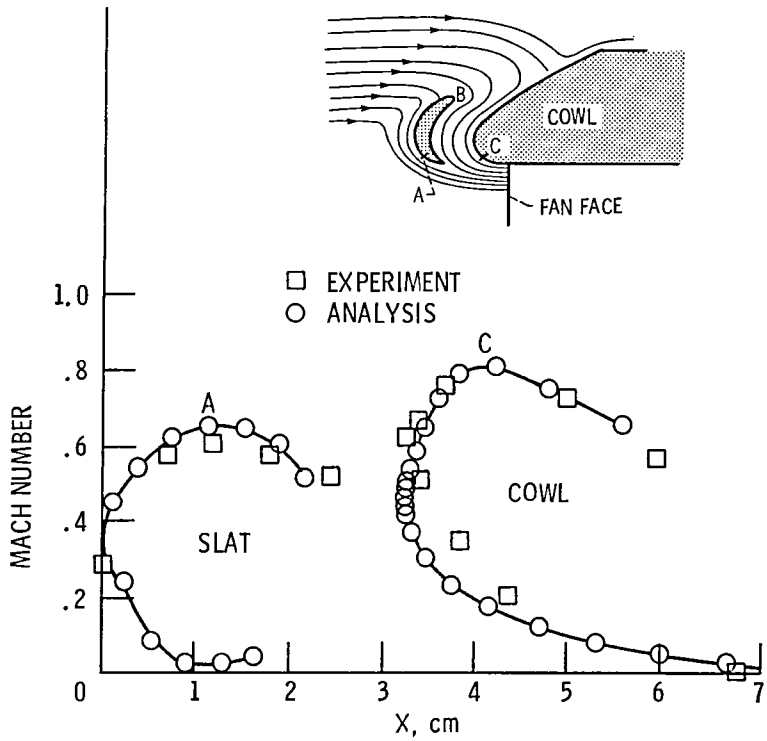

(a) Angle of attack, α, 0^0.

Figure 6. - Comparison of 3-D analysis and experiment, slotted-lip inlet. (M_0 = 0.091; $\dot{m}$ = 14.17 kg/sec.)

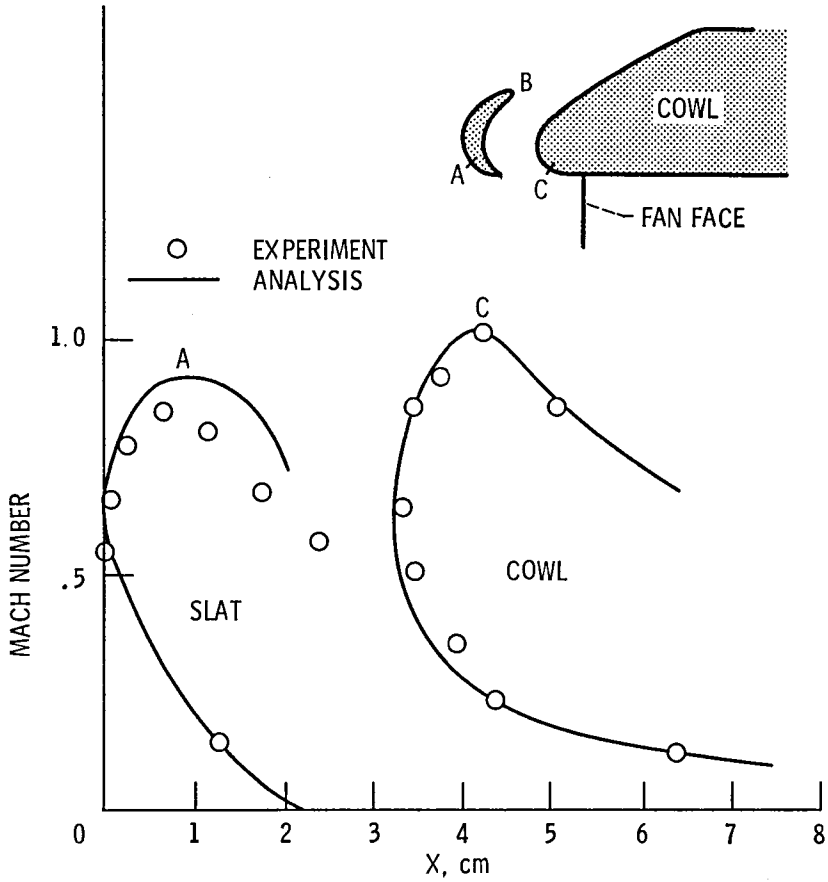

(b) Angle of attack, α, 40^{o}.

Figure 6. - Concluded.

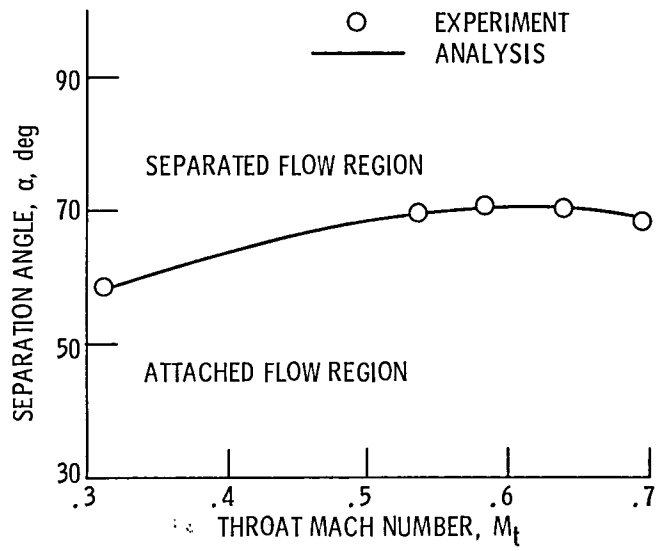

Figure 7. - Separation bound of scarf inlet. (M_0 = 0.18.)

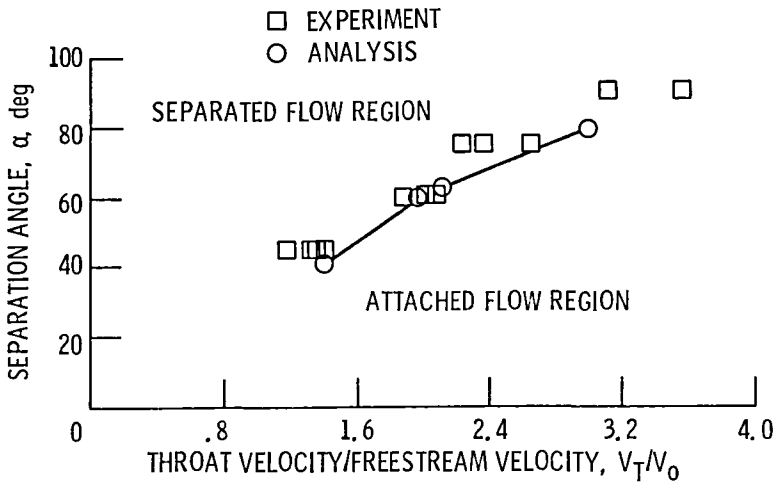

Figure 8. - Separation bound of asymmetric inlet.

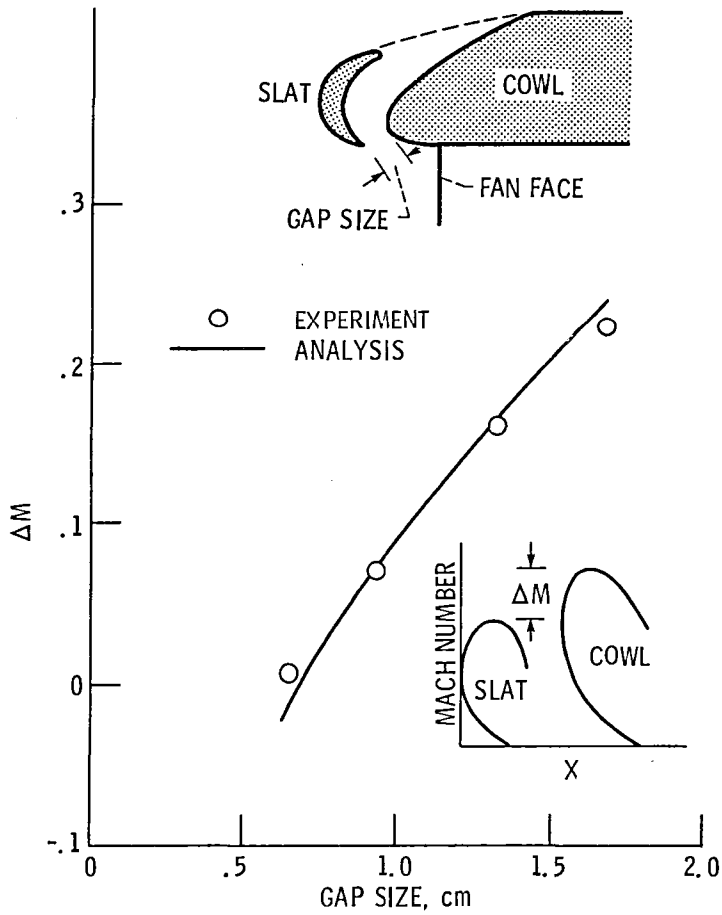

Figure 9. - Comparison of 3-D analysis and experiment for the difference of maximum Mach number between slat and cowl. (M_0 = 0.091.)

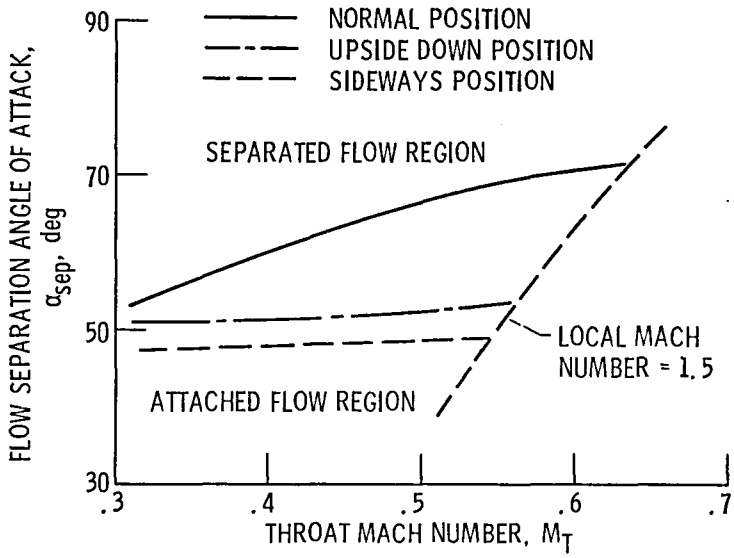

Figure 10. - Separation bound of a scarf inlet in three positions. (M_0 = 0.18.)

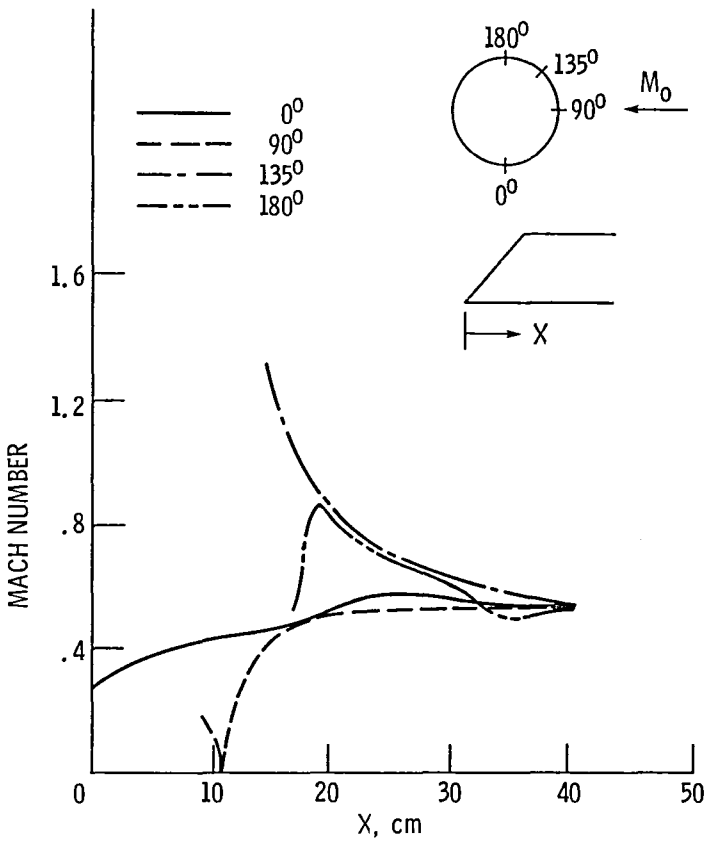

Figure 11. - Surface Mach number along different circumferential positions. (β = 90°; M_0 = 0.18; M_T = 0.54.)

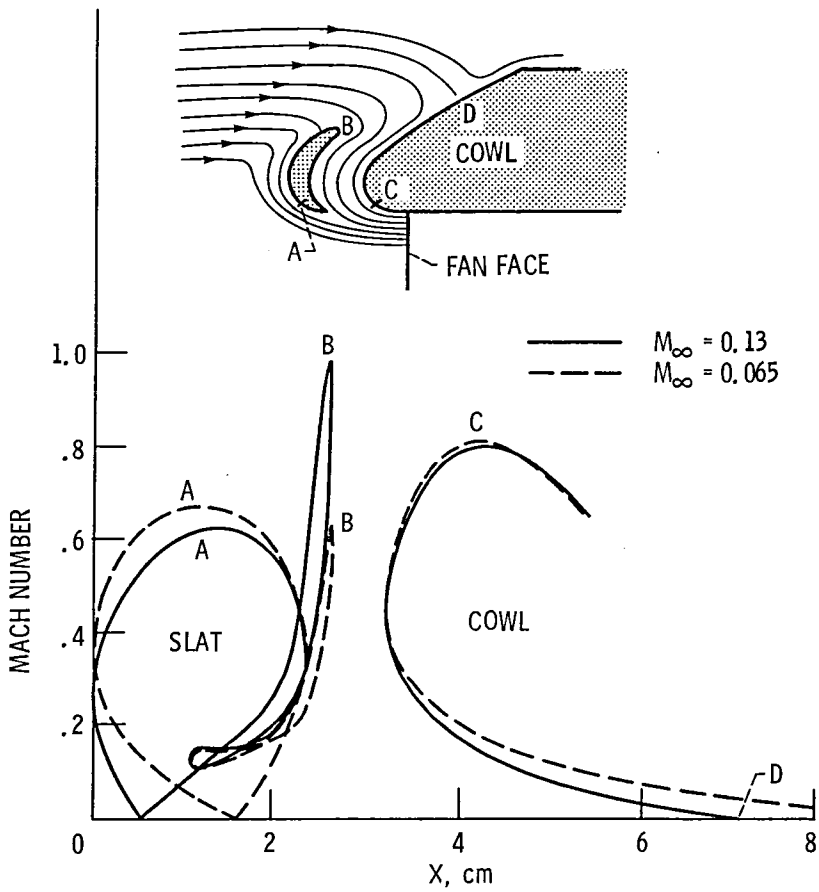

Figure 12. - Effect of freestream Mach number. ($\alpha = 0^0$; $\dot{m}$ = 14.17 kg/sec.)

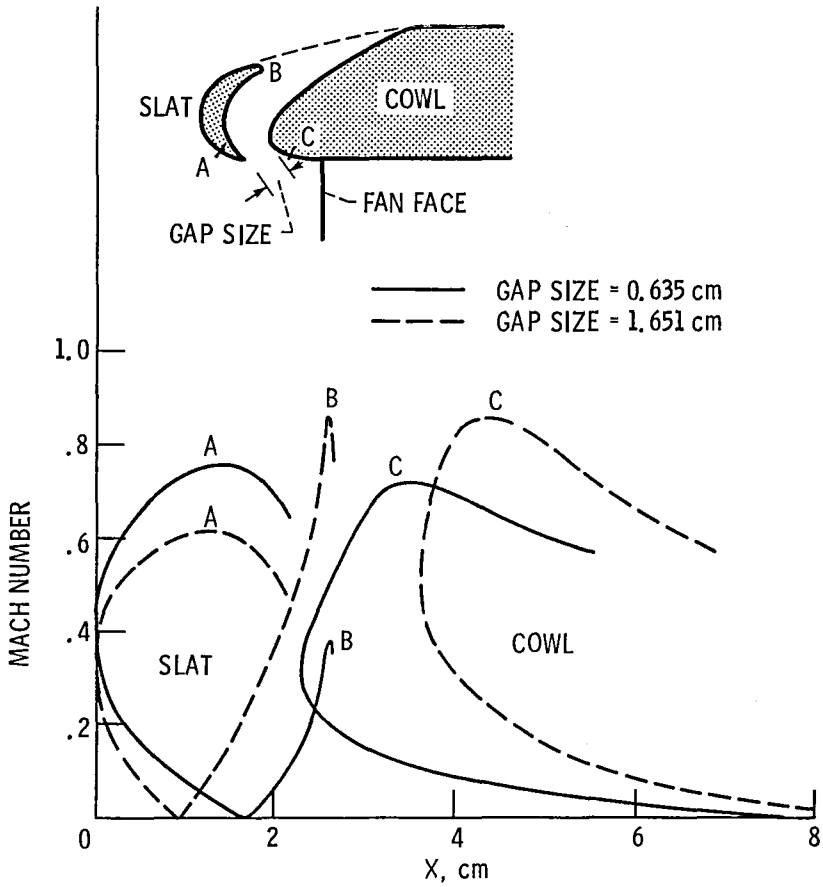

Figure 13. - Effect of gap size. ($\alpha = 0^0$; $M_0 = 0.091$; $\dot{m} = 14.17$ kg/sec.)

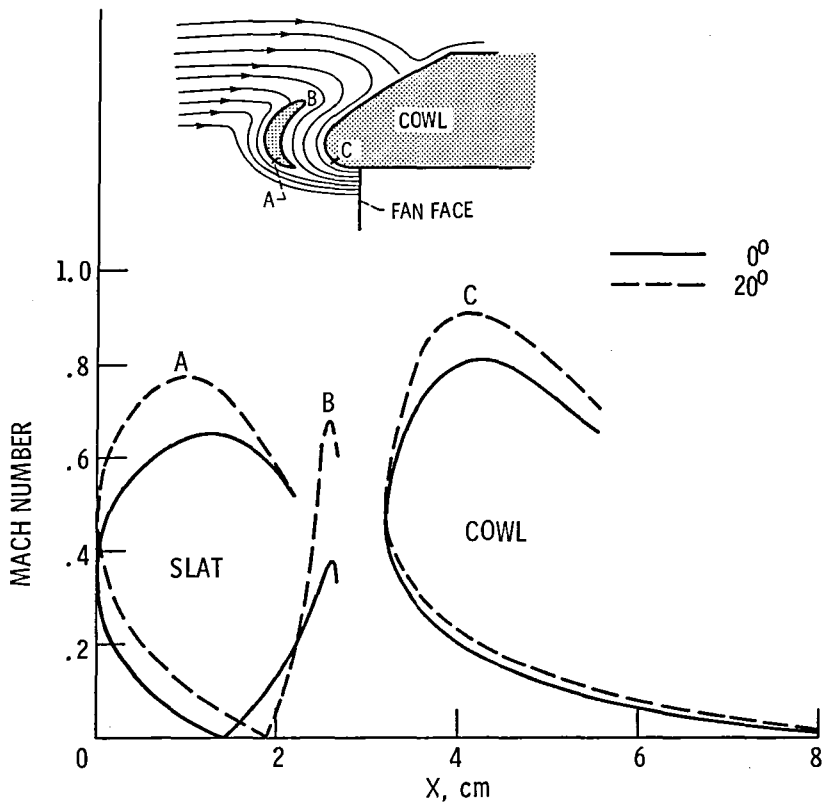

Figure 14. - Effect of angle of attack. (M_0 = 0.091; $\dot{m}$ = 14.17 kg/sec; gap size = 1.3 cm.)

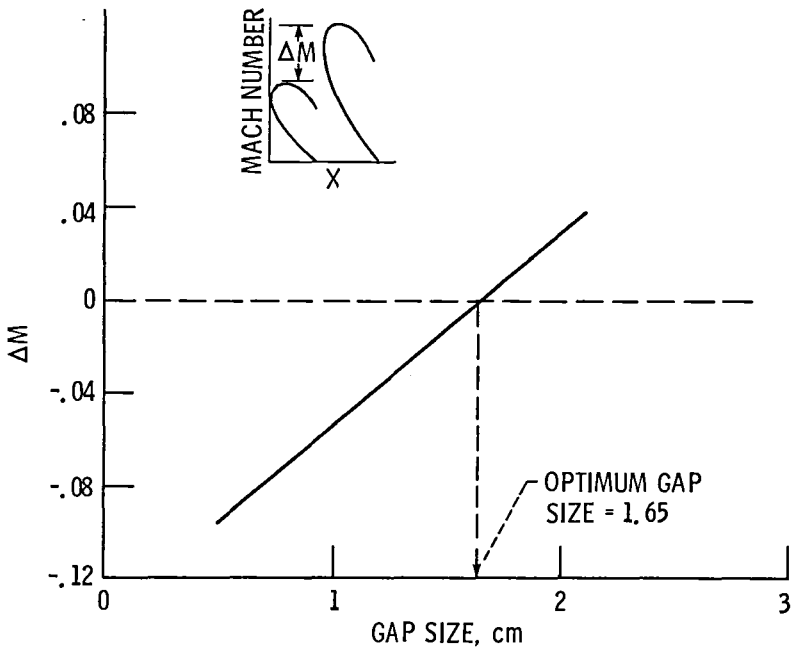

Figure 15. - Optimization of gap size. ($\alpha = 70^0$; $V_0 = 27.7$ m/sec; $V_T = 35.5$ m/sec.)

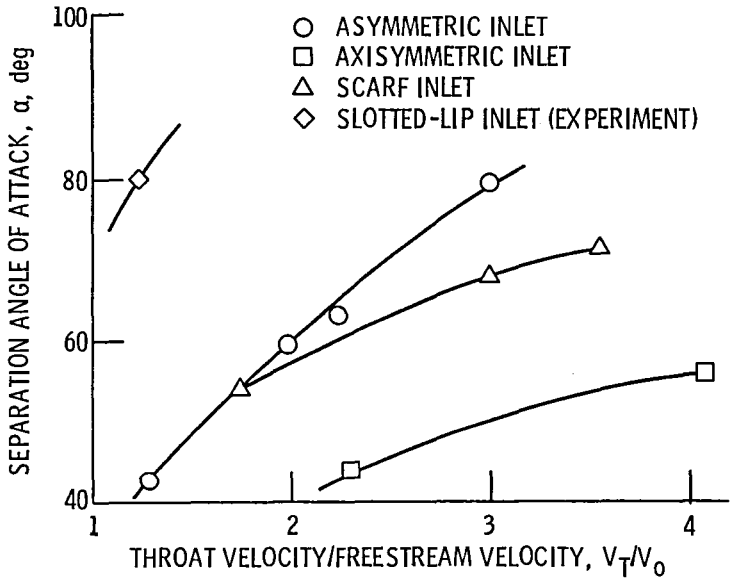

Figure 16. - Comparison of separation bound for various 3-D high angle of attack inlets.

1. Report No. NASA TM-87298 AIAA-86-1627	2. Government Accession No.	3. Recipient's Catalog No.

4. Title and Subtitle	5. Report Date
A Numerical Analysis Applied to High Angle of Attack Three-Dimensional Inlets	6. Performing Organization Code 505-62-91
7. Author(s) Danny P. Hwang	8. Performing Organization Report No. E-3004
	10. Work Unit No.
9. Performing Organization Name and Address National Aeronautics and Space Administration Lewis Research Center Cleveland, Ohio 44135	11. Contract or Grant No.
	13. Type of Report and Period Covered Technical Memorandum
12. Sponsoring Agency Name and Address National Aeronautics and Space Administration Washington, D.C. 20546	14. Sponsoring Agency Code

15. Supplementary Notes

Prepared for the 22nd Joint Propulsion Conference cosponsored by the AIAA, ASME, SAE, and ASEE, Huntsville, Alabama, June 16-18, 1986.

16. Abstract

The three-dimensional analytical methods used to analyze subsonic high angle of attack inlets at the NASA Lewis Research Center are briefly described. The methods are then shown to give good agreement with experimental results for various three-dimensional high angle of attack inlets. Finally, because of this good agreement, the methods have been used to predict aerodynamic characteristics of scarf and slotted-lip inlets. Results of this analytical study are presented.

17. Key Words (Suggested by Author(s))	18. Distribution Statement
Inlet; Analysis; Boundary layer; Propulsion; Potential flow; Separation	Unclassified - unlimited STAR Category 02

19. Security Classif. (of this report)	20. Security Classif. (of this page)	21. No. of pages	22. Price*
Unclassified	Unclassified		

*For sale by the National Technical Information Service, Springfield, Virginia 22161

End of Document